Biochemical and Biophysical Research Communications 461 (2015) 122–127

Contents lists available at ScienceDirect

Biochemical and Biophysical Research Communications

journal homepage: www.elsevier.com/locate/ybbrc

Structural basis for the substrate selectivity of a HAD phosphatase from *Thermococcus onnurineus* NA1

Tri Duc Ngo [a], Binh Van Le [a], Vinod Kumar Subramani [a], Chi My Thi Nguyen [a], Hyun Sook Lee [b], Yona Cho [b], Kyeong Kyu Kim [a, *], Hye-Yeon Hwang [a, *]

[a] Department of Molecular Cell Biology, Samsung Biomedical Research Institute, Sungkyunkwan University School of Medicine, Suwon 440-746, Republic of Korea
[b] Korea Institute of Ocean Science and Technology, Ansan 426-744, Republic of Korea

ARTICLE INFO

Article history:
Received 20 March 2015
Available online 6 April 2015

Keywords:
HAD
Phosphatase
Substrate recognition motif
Crystal structure

ABSTRACT

Proteins in the haloalkaloic acid dehalogenase (HAD) superfamily, which is one of the largest enzyme families, is generally composed of a catalytic core domain and a cap domain. Although proteins in this family show broad substrate specificities, the mechanisms of their substrate recognition are not well understood. In this study, we identified a new substrate binding motif of HAD proteins from structural and functional analyses, and propose that this motif might be crucial for interacting with hydrophobic rings of substrates. The crystal structure of TON_0338, one of the 17 putative HAD proteins identified in a hyperthermophilic archaeon, *Thermococcus onnurineus* NA1, was determined as an apo-form at 2.0 Å resolution. In addition, we determined the crystal structure TON_0338 in complex with Mg^{2+} or N-cyclohexyl-2-aminoethanesulfonic acid (CHES) at 1.7 Å resolution. Examination of the apo-form and CHES-bound structures revealed that CHES is sandwiched between Trp58 and Trp61, suggesting that this Trp sandwich might function as a substrate recognition motif. In the phosphatase assay, TON_0338 was shown to have high activity for flavin mononucleotide (FMN), and the docking analysis suggested that the flavin of FMN may interact with Trp58 and Trp61 in a way similar to that observed in the crystal structure. Moreover, the replacement of these tryptophan residues significantly reduced the phosphatase activity for FMN. Our results suggest that WxxW may function as a substrate binding motif in HAD proteins, and expand the diversity of their substrate recognition mode.

1. Introduction

The haloalkaloic acid dehalogenase (HAD) superfamily is regarded as one of the largest enzyme families [1,2]. Though this family was originally named after haloacid dehalogenases, the majority of members mediate phosphoryl transfer and phosphatases are the most dominant among them [1–3]. HAD phosphatases act on a variety of substrates, but, the biological functions are not known for most of them [4]. Structural and biochemical studies on a number of HAD proteins have provided the atomic basis of their substrate specificity [3]. However, more intensive analyses are necessary to uncover their diversity in substrate-recognition modes and physiological roles.

Structurally characterized HAD phosphatases share a unique HAD fold in the core domain that is characterized by a three-layered α/β sandwich consisting of repeating α/β units [3]. The active site in the core domain is constructed of four loops with consensus motifs (motif I-IV). Motifs I, II, and IV contain key residues involved in nucleophilic attack, phosphoryl group binding, and Mg^{2+} binding, respectively [2,3]. Arg/Lys in Motif III stabilizes the negative charge of the Asp nucleophile and phosphoryl group.

In addition to the core domain, HAD proteins contain a cap domain that is known to mediate substrate binding. HAD proteins are classified into subfamilies C0, C1 and C2 based on the organization and location of cap domains [3]. While C0 structure has very small cap domains, C1 and C2 caps have α-helical bundle and mixed α/β structures of considerable sizes, respectively. The open and

Abbreviations: HAD, haloalkaloic acid dehalogenase; FMN, flavin mononucleotide; CHES, N-cyclohexyl-2-aminoethanesulfonic acid; β-PGM, β-phosphoglucomutase.

* Corresponding authors.
E-mail addresses: kyeongkyu@skku.edu (K.K. Kim), hyhwang3@gmail.com (H.-Y. Hwang).

http://dx.doi.org/10.1016/j.bbrc.2015.03.179
0006-291X/

closed conformations, defined by the relative orientation between the core and cap domains, are required for substrate entry and hydrolysis [5].

The genome analyses of *Thermococcus onnurineus* NA1, a hyperthermophilic archaeon isolated from a deep-sea hydrothermal vent area, revealed 17 putative HAD proteins [6]. Their functions cannot be predicted from the sequence alone, thus structural and biochemical characterizations are necessary. Recent advances in structural genomics provide an opportunity to identify molecular functions of unknown proteins from structural information [7]; these approaches are expected to be applicable to HAD proteins. TON_0338, annotated as one of the HAD phosphatases in *T. onnurineus* NA1, contains four conserved motifs and a C1-type cap domain (Fig. 1). Structural studies of apo-form, Mg^{2+}- and CHES-bound TON_0338, combined with activity assay, revealed that TON_0338 has phosphatase activity with a preference for substrates containing hydrophobic ring moieties. Further docking and mutational analyses confirmed that the WxxW motif in the cap domain is crucial for substrate recognition, suggesting a novel substrate binding mode of HAD phosphatases.

2. Materials and methods

2.1. Protein expression and purification

The cloning and purification methods of the recombinant TON_0338 with a fused C-terminal His tag was described previously [8]. Briefly, The transformed *Escherichia coli* Rosetta(DE3)pLysS was harvested and sonicated in 50 mM Tris–HCl (pH 8.0), 0.5 M KCl, and 10% glycerol. Proteins were purified from the clarified cell lysates using a Hi-Trap chelating column and a Superdex 200 10/300 GL column (Amersham Biosciences) sequentially. The pooled fractions were concentrated using a Centricon YM-10 (Millipore) in 10 mM Tris–HCl (pH 8.0) and 50 mM NaCl. Selenomethionine-substituted protein, expressed in *E. coli* B834(DE3), was prepared in the same way.

2.2. Crystallization and data collection

The initial crystallization screening for native and selenomethionine (SeMet)-substituted TON_0338 proteins was performed by the microbatch crystallization method at 20 °C as described previously [8]. The diffraction-quality crystals of native and SeMet-substituted apo-TON_0338 were obtained using 35% t-butanol and 1.0 M trisodium citrate (pH 5.6). The Mg^{2+}-bound TON_0338 was crystallized using 20% PEG 3000 and 0.1 M citrate (pH 5.5) as precipitant. CHES-bound proteins were crystallized by mixing 1 μl of TON_0338, preincubated with 10 mM glucose 6-phosphate (G6P), with 1 μl of 1.0 M sodium citrate and 0.1 M CHES (pH 9.5). Crystals were transferred to a cryo-solution containing the original precipitant and 25% (v/v) ethylene glycol prior to flash-freezing in a cold nitrogen stream. All diffraction data were collected at beam line 4A of Pohang Accelerator Laboratory, South Korea. The diffraction data from the native, Mg^{2+}- and CHES-bound crystals were collected at 2.0, 1.7, and 1.7 Å resolutions, respectively, using synchrotron radiation at a wavelength of 1.0000 Å. The crystals of apo-TON_0338 belong to monoclinic space group C2 with unit cell $a = 121.2$ Å, $b = 63.0$ Å, $c = 37.5$ Å and $\beta = 106.5°$. The crystals of the

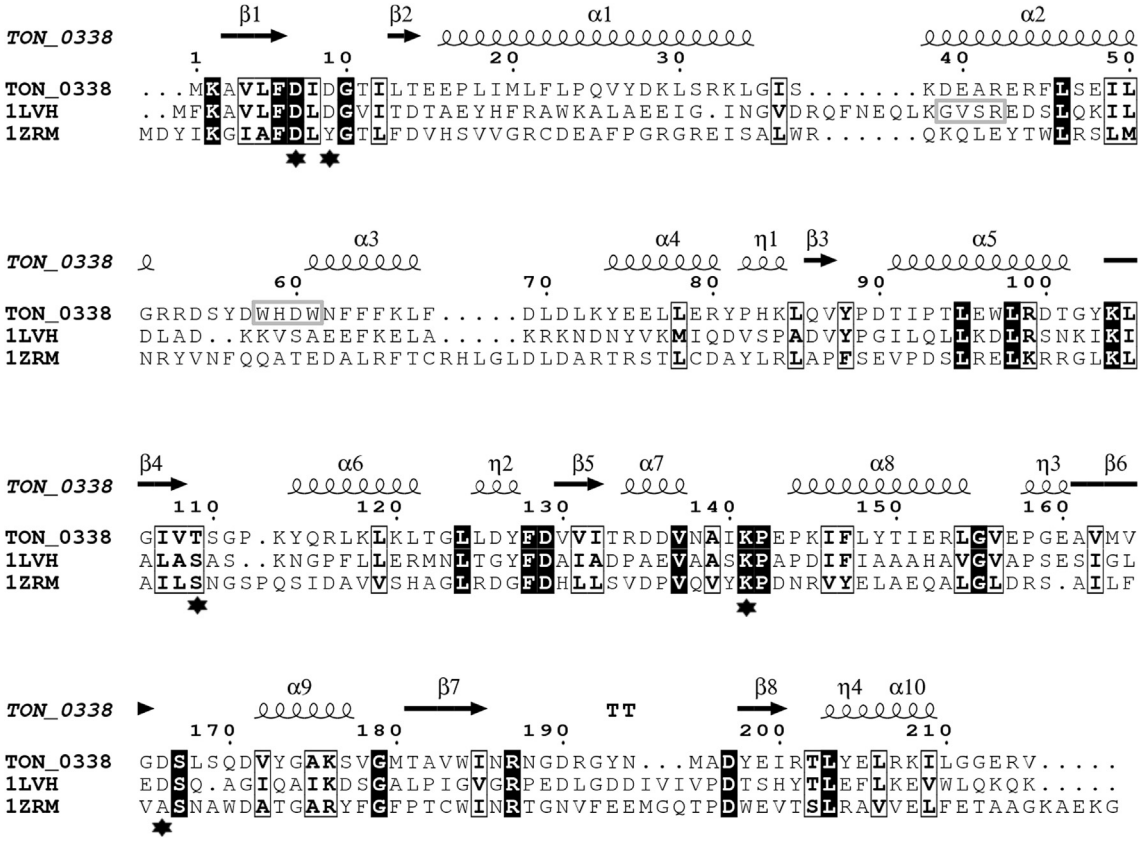

Fig. 1. Sequence alignment of TON_0338 from *Thermococcus onnurineus* NA1, *Lactococcus lactis β-phosphoglucomutase (1LVH)* and *Pseudomonas* sp. YL L-2-haloacid dehalogenase (1ZRM). Secondary structures of TON_0338 are shown above the line. Residues in four catalytic motifs are noted with asterisks. Well-conserved and similar residues are shown as bold white and bold black letters, respectively bold black letters. Stretches of residues that are similar across the group of sequences are shown in boxes. GxxR and WxxW motifs are also indicated with grey boxes.

Mg^{2+}- and CHES-bound TON_0338 also belong to monoclinic space group C2 with similar unit-cell parameters (Table 1). Multiple wavelength anomalous diffraction (MAD) data sets from a monoclinic crystal of SeMet-substituted TON_0338 were collected at three wavelengths, peak (0.9795 Å), edge (0.9796 Å) and remote (0.9718 Å). Data were indexed, integrated, and scaled using HKL2000 [9]. The data statistics are summarized in Table 1.

2.3. Structure determination and refinement

SOLVE and RESOLVE programs were used to trace five selenium sites for phasing and automated model building [10]. Quality of the final map was sufficient for model building. The model was constructed using Coot program [11]. The structure of a complex of TON_0338 with Mg^{2+} or CHES was solved by molecular replacement with the structure of apo-TON_0338 as the template using MOLREP in CCP4 package [12]. The models were refined using Refmac5 [13]. The stereochemistry of the model was checked using Phenix [14]. The refinement statistics are summarized in Table 1. All figures were drawn using Pymol [15].

2.4. Phosphatase activity assay

The phosphatase activity of TON_0338 was assayed with various organic phosphates as substrates using a malachite green phosphate assay kit (Bioassay Systems, Hayward, CA, USA). Briefly, 160 μl reaction mixture containing 0.05–2.0 mM substrate, 50 mM MOPS (pH6.5), 5 mM $MgCl_2$, 100 mM NaCl and 5–10 μg TON_0338 in 96-well microplates were incubated at 80 °C for 10 min. To stop the reaction 40 μl of working malachite green reagent was added and the mixture was incubated at room temperature for color development. The production of P_i was measured by monitoring the absorbance at 620 nm.

2.5. Docking simulation

The Mg^{2+}-bound structure of TON_0338 was used as the template and Trp58 was considered as a flexible residue in the docking procedure. AutoDock Tool [16] was used to prepare the .pdbqt files for both the protein and the ligand. Docking searching space was defined as 20 × 22 × 20 points around the substrate-binding site. Other docking parameters were kept as default. Docking simulation was performed using AutoDock Vina [17]. Among the docking models which had substrates bound to the known active site, the model with the lowest docking energy and reasonable distances between the phosphate group of substrate and the active site residues was used for structure analyses.

3. Results

3.1. Phosphatase activity of TON_0338

The phosphatase activity of TON_0338 was tested on representative metabolic phosphocompounds such as flavin mononucleotide (FMN), phosphotyrosine, glucose-6-phosphate, 6-

Table 1
Data collection and refinement statistics of native, Mg-bound, and CHES-bound TON_0338.

	TON_0338	Mg-TON_0338	CHES-TON_0338	SelMet TON_0338		
Data collection						
Space group	C2	C2	C2	C2		
Cell dimensions						
a, *b*, *c* (Å)	121.2, 63.0, 37.5	122.4, 61.3, 37.4	122.5, 61.7, 37.6	122.5, 62.6, 37.4		
β (°)	106.5	107.4	107.4	106.9		
				Peak	Inflection	Remote
Wavelength	1.0000	1.0000	1.0000	0.9795	0.9796	0.9718
Resolution (Å)	50–2.0 (2.07–2.0)	30–1.7 (1.76–1.7)	30–1.7 (1.73–1.7)	50–2.45 (2.07–2.0)	50–2.45 (2.07–2.0)	50–2.45 (2.07–2.0)
R_{merge}[a]	8.9 (26.2)	6.1 (25.9)	6.5 (33.9)	8.1 (14.1)	7.0 (14.0)	7.7 (17.7)
$\langle I\rangle/\langle\sigma I\rangle$	17.8 (5.3)	19.8 (4.03)	21.7 (2.7)	39.2 (12.7)	36.9 (10.8)	35.3 (8.8)
Completeness (%)	94.7 (93.1)	98.9 (98.5)	98.3 (95.1)	98.2 (90.2)	97.7 (86.1)	99.1 (97.3)
Redundancy	3.1 (2.6)	2.5 (2.5)	3.5 (3.4)	3.5	3.7	3.7
Measured reflections	54,607	72,422	100,744			
Unique reflections	17,464 (1691)	28,855 (2854)	28,848 (1390)			
Refinement						
Resolution (Å)	33–2.0	29.2–1.7	29.2–1.7			
No. reflections	17,464	28,854	28,848			
R_{work}[b]/R_{free}	0.166/0.202	0.156/0.196	0.162/0.188			
No. atoms						
Protein	1794	1868	1861			
Ligand/ion	5/0	14/1	27/1			
Water	130	156	198			
B-factors (Å^2)						
Protein	26.4	16.6	19.6			
Ligand/ion	35.7/–	19.8/13.2	21.6/14.8			
R.M.S.D[c]						
Bond lengths (Å)	0.007	0.006	0.007			
Bond angles (°)	1.040	1.180	1.060			
Ramachandran						
Favored (%)	99.08	98.26	98.68			
Outliers (%)	0	0	0.97			

[a] $R_{merge=\sum h}\sum_i|I(h_i)-<I(h)>|/\sum_h\sum_i I(h_i)$, where $I(h_i)$ is the single intensity of reflection *h* as determined by the *i*th measurement and $\langle I(h)\rangle$ is the mean intensity of reflections *h*.

[b] $R_{work}(\%)=\sum|Fo|-|Fc|/\sum Fo$, where, *Fo* is the observed structure factor amplitude, and *Fc* is the structure factor calculated from the model.

[c] R.M.S.D. has been calculated from the values used in Phenix [14].

phosphogluconate and 3-phosphoglycerate. Among them, FMN turned out to be the most preferred substrate (Table 2).

3.2. Overall fold of TON_0338

The final model of apo-TON_0338, comprising all residues except residues 216–226, was refined at 2.0 Å with an R_{factor} of 0.166 and an R_{free} of 0.202 (Table 1). PISA analysis of the TON_0338 structure suggested that the protein is monomeric [18], consistent with its oligomerization status predicted from the gel-filtration profile (data not shown). TON_0338 is composed of a cap domain with a four-helix bundle and a core domain with a three-layered α/β sandwich fold, thus is classified into C1 subfamily of HAD phosphatases [3] (Fig. 2). As found in other HAD proteins, the core domain of TON_0338 (residues 1–12 and 88–216) has a modified Rossmann fold that is composed of a six-stranded parallel β-sheet (β1, β4, β5, β6, β7, β8) surrounded by four helices (α5–α8). The cap domain (residues 13–87), placed between the strand β1 and the helix α5 of the core domain, contains a four-helical bundle (α1–α4) and a small two-stranded anti-parallel β-sheet. The active site of TON_0338 is located at the interface of core and cap domains. The volume of the cavity formed between two domains is 444 $Å^3$, which can accommodate phosphorylated substrates like FMN (estimated volume = 366 $Å^3$).

Similar to other known HAD proteins [3], in its active site TON_0338 contains key residues involved in substrate binding and catalysis: Asp7, a nucleophile; Thr109 for phosphate binding; Lys141 for stabilization of Asp7 and phosphate groups; and Asp166 for magnesium ion binding (Figs. 1 and 2). In the Mg^{2+}-bound structure (Fig. 2D), the magnesium ion is in a hexagonal geometry coordinated by three Asp residues (Asp7, Asp9 and Asp 166) and three water molecules (W1, W2 and W3).

To understand the substrate specificity of TON_0338 at molecular level, we attempted crystallization in the presence of various substrates. During these attempts, a long electron density was identified in the substrate-binding site, which was later modeled as CHES, considering the reagents used for the crystallization and the shape of electron density (Fig. 3). This structure, designated as the CHES-bound structure, was further analyzed.

3.3. Structural comparison with other known HAD phosphatases

We searched for similar structures of TON_0338 in the DALI server. Among homologous protein structures with defined functions, *Pseudomonas* sp. YL L-2-haloacid dehalogenase (1ZRM) [19] and *Lactococcus lactis* β-phosphoglucomutase (β-PGM: 1LVH) [20] showed the highest degree of similarity with Z-scores of 23.4 and 19.7, respectively. Of these, TON_0338 was compared to β-PGM which facilitates the interconversion of glucose 1-phosphate and glucose 6-phosphate, since both have conserved catalytic residues (Fig. 1) and bind to phosphorylated compounds. β-PGM has 24.4% sequence identity with TON_0338, and its crystal structures has been solved in apo- [21], intermediate-bound [5,20] and inhibitor-bound forms [5]. β-PGM was shown to undergo conformational changes from open to closed conformations upon substrate binding

Table 2
Phosphatase activity of wild-type and W58A/W61A TON_0338 toward different substrates.

	Wild-type (%)[a]	W58A/W61A (%)[a]
FMN	100	4.24
pTyr	3.27	0.40
G6P	2.33	0.68
6PG	1.04	0.23
3PG	0.69	0.36

[a] The phosphatase activity was measured using the malachite green method and represented as the percentage relative to the activity of wild type TON_0338 for FMN. FMN: flavin mononucleotide, pTyr: phosphotyrosine, G6P: glucose-6-phosphate, 6PG: 6-phosphogluconate, 3PG: 3-phosphoglycerate.

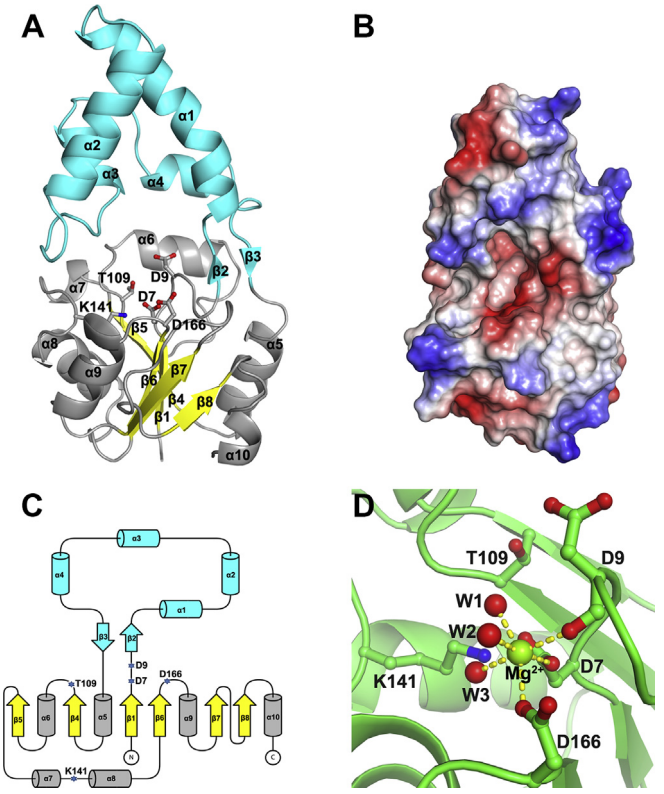

Fig. 2. Crystal structure of TON_0338. (A) Schematic representation of the structure of TON_0338. The core domain is colored grey and yellow, and the cap domain is colored cyan. (B) Surface representation of TON_0338. The electrostatic surface potential calculated using the program Pymol was contoured at −100 kT (red, most negative) and +100 kT (blue, most positive). (C) Topology representation of TON_0338. β-Strands and α-helices are shown as arrows and cylinders, respectively. Conserved catalytic residues are indicated. (D) The active site of TON_0338. Hydrogen bonds are shown as yellow dashed lines. Mg^{2+} and water molecules are shown as green and red spheres, respectively. Catalytic and Mg^{2+} coordinating residues are indicated.

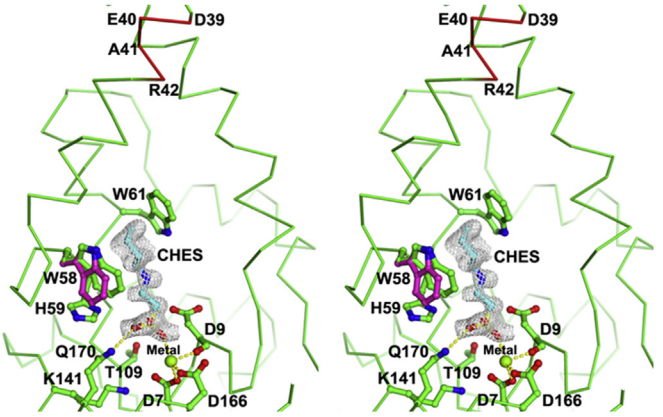

Fig. 3. Stereoview of the active site of CHES [2-(cyclohexylamino)ethanesulfonic acid]-bound TON_0338. Shown in magenta is Trp58 in apo-TON_0338. Important residues and CHES are depicted as ball and stick models. W58 and W61 as well as the residues corresponding to GxxR of β-PGM (D46-E47-A48-R49) are also indicated. Metal is depicted as a green sphere (Metal). Hydrogen bonds are shown as yellow dashed lines.

[21]. TON_0338 overlaps with the closed and open form of β-PGM with rmsd of 3.2 and 3.1 Å, respectively (Figs. 4 and S1). The core domain of TON_0338, including the Mg^{2+} binding site and catalytic residues, are similar to those in both forms of β-PGM. However, they differ in the size and topology of cap domains (Figs. 4 and S1), which are known to be involved in substrate recognition of the C1 subfamily by constituting one side of the substrate-binding pocket in the closed conformation [22]. The most prominent difference is found in helices α2 and α3 of TON_0338 (Figs. 4 and S1). Helix α2 of the TON_0338 cap domain is longer and is connected to helix α3 through a longer loop. This loop creates a bigger surface interface and increases the volume of the cavity. The helices α3 and α4 of TON_0338 are shorter than those in β-PGM, though this does not affect the cavity volume.

It was suggested that in β-PGM, the closure of the cap domain is achieved by the rigid motion between two domains upon substrate binding [21]. It is proposed that GxxR motif in the β-PGM subfamily performs a key role in recognizing substrates [3]. Accordingly, Arg49 in the GxxR motif of β-PGM from *Lactococcus lactis* (Gly46-Val47-Ser48-Arg49, Fig. 1) approaches toward the active site about 6 Å during interdomain conformational change. However, the corresponding residues in TON_0338 (Asp39-Glu40-Ala41-Arg42, Fig. 1) do not appear to structurally overlap with Gly46-Val47-Ser48-Arg49 of β-PGM (Figs. 3 and 4 and S1).

3.4. CHES-bound structure of TON_0338

The sulfonic group of CHES coordinates the metal ion and forms a hydrogen bond with Gln170 (Fig. 3). The most notable finding was the rotation of Trp58 toward CHES in the binding pocket. Consequently, Trp58 and Trp61 form a sandwich structure that makes a tight hydrophobic packing with the cyclohexyl ring of CHES. This observation suggests that the tryptophan sandwich might be a binding motif that interacts with hydrophobic moiety of substrates. This suggestion was supported by the result that TON_0338 showed high phosphatase activity for FMN (Table 2). Interestingly, the Trp58-His59-Asp60-Trp61 of TON_0338 are located near the position where the GxxR motif of β-PGM is found, when cap domains of both proteins are superimposed (Fig. 4 and S1). Therefore, we hypothesized that WxxW is a novel substrate-recognition motif in HAD proteins that is functionally comparable to the GxxR motif in β-PGM. This possibility was verified by modeling of the FMN-bound structure and activity assay of Trp mutants.

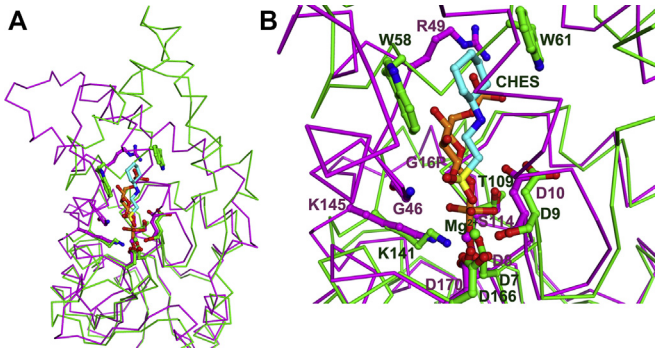

Fig. 4. Superposition of TON_0338 with the closed form of *Lactococcus lactis* β-phosphoglucomutase (β-PGM). (A) The entire Cα-traces of TON_0338 (green) and β-PGM (magenta). (B) Close up view of the substrate-binding site. CHES and glucose-1,6-bisphosphate (G16P) are colored cyan and orange, respectively. Important residue of TON_0338 (black) and β-PGM (magenta) are indicated.

3.5. Docking analysis with FMN

FMN was docked into the putative substrate-binding pocket of TON_0338 to investigate the binding mode of ligands to the active site and the role of the WxxW motif. Trp58 was set as a flexible residue. In the docking model, FMN fits well into the substrate-binding pocket located at the interface between two domains. The phosphate group of FMN was buried inside the active site where O1P makes a hydrogen bond with Thr109 and O3P interacts with Mg^{2+} (Fig. S2). The flavin moiety of FMN is packed into the pocket formed by Thr14, Glu15, Glu16, Ile1 9, Ile49, Trp58, His59 and Trp61. Trp58 and Trp61 were shown to form a sandwich structure with flavin, as in the crystal structure.

3.6. Structure-based mutagenesis

Both the CHES-bound structure and the FMN-bound docking model suggested that two tryptophan residues are involved in substrate recognition. To investigate their role in phosphatase activity, the activity of the double-tryptophan mutant W58A/W61A was examined (Table 2). Though the mutant showed reduced activity for all the tested substrates, its activity for FMN was reduced to the greatest extent (~95%).

4. Discussion

In an attempt to identify the biochemical role of TON_0338, we solved its crystal structures in three different forms: apo-form, Mg^{2+}- and CHES-complexes. TON_0338 is structurally similar to other HAD phosphatases despite low sequence homology. When CHES-bound TON-0338 was compared with β-PGM complexed with glucose-1,6-bisphosphate, it was revealed that WxxW motif of TON_0338 is located inside the turn region of helix2-turn-helix3 of the cap domain, analogous to GxxR motif of β-PGM which recognizes substrates (Fig. 4 and S1). Moreover, the WxxW motif seems to interact with hydrophobic moieties of substrates by forming a tryptophan sandwich structure; the phosphatase activity assay showed that TON_0338 has a preference for substrates containing a hydrophobic ring structure such as FMN. The NCBI BLAST search for non-redundant protein sequences revealed other HAD proteins with the WxxW motif (Table 3), suggesting that it might be a new substrate-binding motif in HAD phosphatases.

Although WxxW of TON_0338 appears to be functionally comparable to GxxR of β-PGM [22], it could not be inferred from the sequence alignment. As substrate recognition motifs cannot be defined simply from sequence alignment, it is necessary to determine three-dimensional structures in order to predict substrate specificity and the residues constituting substrate-binding sites. The cap domain of β-PGM moves toward the active site when it switches from the open to the closed structure forming a glucose recognition motif. It is not clear if TON_0338 similarly has two conformational states, and if the current CHES-bound structure represents the active conformation. But, it is possible that the current CHES-bound model represents the substrate-bound structure and WxxW motif plays a role in substrate recognition of TON_0338, considering the structural conservation of key catalytic residues, analogous positions of GxxR and WxxW motifs, and structural superposition of D-glucose 1,6-bisphosphate and CHES (Fig. 4). The substrate preference of TON_0338 and the effect of Trp-to-Ala mutation also propose WxxW motif as a substrate filter. Collectively, the structure-based elucidation of the mode of substrate recognition, combined with phosphatase assays of wild-type and mutant proteins, implies that WxxW motif has a unique tryptophan sandwich structure and functions as a new substrate-recognition motif in HAD proteins.

Table 3
List of TON_0338 homologues containing the WxxW motif.

NCBI Accession	Name	Species	Sequence identity
YP_004762287.1	Hydrolase	*Thermococcus* sp. 4557	82%
YP_006424368.1	Hypothetical protein with HAD-like domain 2	*Thermococcus* sp. CL1	83%
YP_182890.1	HAD superfamily hydrolase	*Thermococcus kodakarensis* KOD1	75%
YP_004070956.1	2-haloalkanoic acid dehalogenase	*Thermococcus barophilus* MP	70%
YP_002582440.1	HAD-superfamily hydrolase	*Thermococcus* sp. AM4	72%
YP_002960255.1	HAD superfamily hydrolase	*Thermococcus gammatolerans* EJ3	71%
YP_002993845.1	Hydrolase, HAD superfamily	*Thermococcus sibiricus* MM 739	66%
ZP_11215238.1	HAD superfamily hydrolase	*Thermococcus zilligii* AN1	66%
ZP_09729543.1	Hydrolase, HAD superfamily protein	*Thermococcus litoralis* DSM 5473	64%
YP_004624248.1	Hydrolase	*Pyrococcus yayanosii* CH1	60%
NP_143765.1	Hypothetical protein PH1936	*Pyrococcus horikoshii* OT3	59%
NP_127386.1	Hypothetical protein PAB1224	*Pyrococcus abyssi* GE5	59%
YP_006354055.1	Hydrolase related to 2-haloalkanoic acid dehalogenase	*Pyrococcus* sp. ST04	55%
YP_004423790.1	Hypothetical protein PNA2_0870	*Pyrococcus* sp. NA2	56%
NP_577951.1	Hydrolase related to 2-haloalkanoic acid dehalogenase	*Pyrococcus furiosus* DSM 3638	53%

4.1. Accession numbers

The atomic coordinates and structure factors were deposited in the Protein Data Bank, www.pdb.org (PDB ID codes 4YGQ, 4YGS and 4YGR for apo-form, Mg^{2+}-bound, and CHES-bound structures of TON_0338, respectively).

Acknowledgments

This work was supported by Agriculture, Food and Rural Affairs Research Center Support Program, Ministry of Agriculture, Food and Rural Affairs, National Research Foundation of Korea grant to KKK (2011-0028878), HYH (2012R1A1A3010753) and HSL (PM57720). The authors also thank Dr. N K Lokanath for his comments on the structures.

Appendix A. Supplementary data

Supplementary data related to this article can be found at http://dx.doi.org/10.1016/j.bbrc.2015.03.179.

Transparency document

Transparency document related to this article can be found online at http://dx.doi.org/10.1016/j.bbrc.2015.03.179.

References

[1] K.N. Allen, D. Dunaway-Mariano, Phosphoryl group transfer: evolution of a catalytic scaffold, Trends Biochem. Sci. 29 (2004) 495–503.
[2] E.V. Koonin, R.L. Tatusov, Computer analysis of bacterial haloacid dehalogenases defines a large superfamily of hydrolases with diverse specificity. Application of an iterative approach to database search, J. Mol. Biol. 244 (1994) 125–132.
[3] A.M. Burroughs, K.N. Allen, D. Dunaway-Mariano, L. Aravind, Evolutionary genomics of the HAD superfamily: understanding the structural adaptations and catalytic diversity in a superfamily of phosphoesterases and allied enzymes, J. Mol. Biol. 361 (2006) 1003–1034.
[4] E. Kuznetsova, M. Proudfoot, C.F. Gonzalez, G. Brown, M.V. Omelchenko, I. Borozan, L. Carmel, Y.I. Wolf, H. Mori, A.V. Savchenko, C.H. Arrowsmith, E.V. Koonin, A.M. Edwards, A.F. Yakunin, Genome-wide analysis of substrate specificities of the Escherichia coli haloacid dehalogenase-like phosphatase family, J. Biol. Chem. 281 (2006) 36149–36161.
[5] D.S. Lahiri, G. Zhang, D. Dunaway-Mariano, K.N. Allen, The pentacovalent phosphorus intermediate of a phosphoryl transfer reaction, Science 299 (2003) 2067–2071.
[6] S.S. Bae, Y.J. Kim, S.H. Yang, J.K. Lim, J.H. Jeon, H.S. Lee, S.G. Kang, S.J. Kim, J.-H. Lee, Thermococcus onnurineus sp. nov., a hyperthermophilic archaeon isolated from a deep-sea hydrothermal vent area at the PACMANUS field, J. Microbiol. Biotechnol. 16 (2006) 1826–1831.
[7] T.I. Zarembinski, L.W. Hung, H.J. Mueller-Dieckmann, K.K. Kim, H. Yokota, R. Kim, S.H. Kim, Structure-based assignment of the biochemical function of a hypothetical protein: a test case of structural genomics, Proc. Natl. Acad. Sci. U.S.A. 95 (1998) 15189–15193.
[8] C.M. Nguyen, H.S. Lee, Y. Cho, J.H. Lee, S.C. Ha, H.Y. Hwang, K.K. Kim, Crystallization and preliminary X-ray studies of TON_0559, a putative member of the haloacid dehalogenase (HAD) superfamily from Thermococcus onnurineus NA1, Protein Pept. Lett. 15 (2008) 235–237.
[9] Z. Otwinowski, W. Minor, Processing of x-ray diffraction data collected in Oscillation mode, Methods Enzymol. 276 (1997) 307–326.
[10] T.C. Terwilliger, SOLVE and RESOLVE: automated structure solution, density modification, and model building, J. Synchrotron Radiat. (2004) 49–52.
[11] P. Emsley, B. Lohkamp, W.G. Scott, K. Cowtan, Features and development of Coot, Acta Crystallogr. D66 (2006) 486–501.
[12] M.D. Winn, C.C. Ballard, K.D. Cowtan, E.J. Dodson, P. Emsley, P.R. Evans, R.M. Keegan, E.B. Krissinel, A.G. Leslie, A. McCoy, S.J. McNicholas, G.N. Murshudov, N.S. Pannu, E.A. Potterton, H.R. Powell, R.J. Read, A. Vagin, K.S. Wilson, Overview of the CCP4 suite and current developments, Acta Crystallogr. D67 (2011) 235–242.
[13] A.A. Vagin, R.A. Steiner, A.A. Lebedev, L. Potterton, S. McNicholas, F. Long, G.N. Murshudov, REFMAC5 dictionary: organization of prior chemical knowledge and guidelines for its use, Acta Crystallogr. D60 (2004) 2184–2195.
[14] P.D. Adams, P.V. Afonine, G. Bunkoczi, V.B. Chen, I.W. Davis, N. Echols, J.J. Headd, L.W. Hung, G.J. Kapral, R.W. Grosse-Kunstleve, A.J. McCoy, N.W. Moriarty, R. Oeffner, R.J. Read, D.C. Richardson, J.S. Richardson, J.T.C. Terwilliger, P.H. Zwart, PHENIX: a comprehensive Python-based system for macromolecular structure solution, Acta Crystallogr. D66 (2010) 213–221.
[15] W.L. DeLano, The PyMOL Molecular Graphic System, DeLano Scientific, Palo Alto, CA, 2002.
[16] G.M. Morris, R. Huey, W. Lindstrom, M.F. Sanner, R.K. Belew, D.S. Goodsell, A.J. Olson, AutoDock4 and AutoDockTools4: automated docking with selective receptor flexibility, J. Comput. Chem. 30 (2009) 2785–2791.
[17] O. Trott, A.J. Olson, AutoDock Vina: improving the speed and accuracy of docking with a new scoring function, efficient optimization, and multithreading, J. Comput. Chem. 31 (2010) 455–461.
[18] E. Krissinel, K. Henrick, Inference of macromolecular assemblies from crystalline state, J. Mol. Biol. 372 (2007) 774–797.
[19] Y.F. Li, Y. Hata, T. Fujii, T. Hisano, M. Nishihara, T. Kurihara, N. Esaki, Crystal structures of reaction intermediates of L-2-haloacid dehalogenase and implications for the reaction mechanism, J. Biol. Chem. 273 (1998) 15035–15044.
[20] S.D. Lahiri, G. Zhang, D. Dunaway-Mariano, K.N. Allen, Caught in the act: the structure of phosphorylated beta-phosphoglucomutase from Lactococcus lactis, Biochemistry 41 (2002) 8351–8359.
[21] G. Zhang, J. Dai, L. Wang, D. Dunaway-Mariano, L.W. Tremblay, K.N. Allen, Catalytic cycling in beta-phosphoglucomutase: a kinetic and structural analysis, Biochemistry 44 (2005) 9404–9416.
[22] S.D. Lahiri, G. Zhang, J. Dai, D. Dunaway-Mariano, K.N. Allen, Analysis of the substrate specificity loop of the HAD superfamily cap domain, Biochemistry 43 (2004) 2812–2820.